Linking Transient Voltage to Spatially-Resolved Luminescence Imaging to Understand Reliability of Perovskite Photovoltaics

Preprint

Yasas Patikirige,[1,2] Dana B. Sulas-Kern,[2] Marco Nardone,[3] Steve Johnston,[2] Chuanxiao Xiao,[2] Harvey Guthrey,[2] Kai Zhu,[2] Fei Zhang,[2] and Mowafak Al-Jassim[2]

1 Colorado School of Mines
2 National Renewable Energy Laboratory
3 Bowling Green State University

Presented at the 48th IEEE Photovoltaic Specialists Conference (PVSC 48)
June 20-25, 2020

NREL is a national laboratory of the U.S. Department of Energy
Office of Energy Efficiency & Renewable Energy
Operated by the Alliance for Sustainable Energy, LLC

This report is available at no cost from the National Renewable Energy Laboratory (NREL) at www.nrel.gov/publications.

Contract No. DE-AC36-08GO28308

Conference Paper
NREL/CP-5K00-80422
July 2021

Linking Transient Voltage to Spatially-Resolved Luminescence Imaging to Understand Reliability of Perovskite Photovoltaics

Preprint

Yasas Patikirige,[1,2] Dana B. Sulas-Kern,[2] Marco Nardone,[3] Steve Johnston,[2] Chuanxiao Xiao,[2] Harvey Guthrey,[2] Kai Zhu,[2] Fei Zhang,[2] and Mowafak Al-Jassim[2]

1 Colorado School of Mines
2 National Renewable Energy Laboratory
3 Bowling Green State University

Suggested Citation
Patikirige, Yasas, Dana B. Sulas-Kern, Marco Nardone, Steve Johnston, Chuanxiao Xiao, Harvey Guthrey, Kai Zhu, Fei Zhang, and Mowafak Al-Jassim. 2021. *Linking Transient Voltage to Spatially-Resolved Luminescence Imaging to Understand Reliability of Perovskite Photovoltaics: Preprint*. Golden, CO: National Renewable Energy Laboratory. NREL/CP-5K00-80422. https://www.nrel.gov/docs/fy21osti/80422.pdf.

NREL is a national laboratory of the U.S. Department of Energy
Office of Energy Efficiency & Renewable Energy
Operated by the Alliance for Sustainable Energy, LLC

This report is available at no cost from the National Renewable Energy Laboratory (NREL) at www.nrel.gov/publications.

Contract No. DE-AC36-08GO28308

Conference Paper
NREL/CP-5K00-80422
July 2021

National Renewable Energy Laboratory
15013 Denver West Parkway
Golden, CO 80401
303-275-3000 • www.nrel.gov

NOTICE

This work was authored in part by the National Renewable Energy Laboratory, operated by Alliance for Sustainable Energy, LLC, for the U.S. Department of Energy (DOE) under Contract No. DE-AC36-08GO28308. Funding provided by the U.S. Department of Energy Office of Energy Efficiency and Renewable Energy Solar Energy Technologies Office. The views expressed herein do not necessarily represent the views of the DOE or the U.S. Government. The U.S. Government retains and the publisher, by accepting the article for publication, acknowledges that the U.S. Government retains a nonexclusive, paid-up, irrevocable, worldwide license to publish or reproduce the published form of this work, or allow others to do so, for U.S. Government purposes.

Cover Photos by Dennis Schroeder: (clockwise, left to right) NREL 51934, NREL 45897, NREL 42160, NREL 45891, NREL 48097, NREL 46526.

Linking Transient Voltage to Spatially-Resolved Luminescence Imaging to Understand Reliability of Perovskite Photovoltaics

Yasas Patikirige[1,2], Dana B. Sulas-Kern[2] , Marco Nardone[3], Steve Johnston[2], Chuanxiao Xiao[2], Harvey Guthrey[2], Kai Zhu[2], Fei Zhang[2], Mowafak Al-Jassim[2]

[1]Colorado School of Mines, Golden, CO, 80401, U.S.A.
[2]National Renewable Energy Laboratory, Golden, CO, 80401, U.S.A.
[3]Bowling Green State University, Bowling Green, OH, 43403, U.S.A.

***Abstract*—In this work, we present a methodology to separate effects of perovskite device metastability from irreversible degradation, using stress/rest cycling under constant current bias while collecting a series of electroluminescence images and continuously monitoring voltage. We develop a simulation model and procedures for image processing to better understand the effects of ion parameters on the transient nature of voltage and evolving electroluminescence images.**

I. Introduction

With a record efficiency of 25.5% [1], perovskite solar cells have attracted attention among the photovoltaics community. Unlike traditional photovoltaic semiconductors, halide perovskite materials exhibit strong ionic contributions that are influenced by electrical bias [2][3]. Different phenomena have been used to explain anomalous behavior in perovskites, including the impacts of electron/hole trapping/de-trapping, ion migration, slow transient capacitive current, and ferroelectric polarization [3-5]. These effects are often reversible under different bias conditions and time scales, which can cause the well-known effects of current-voltage hysteresis. However, reaching long-term reliability and commercialization depends on separately understanding such reversible changes as well as the extent to which related processes can cause irreversible degradation.

The race to perovskite commercialization is driving greater interest in stability testing and rationally-designed pathways to enhance reliability. Here, we present methods to characterize perovskite (meta)stability and to analyze the extents of varying charging and mobile ion parameters. We accomplish this through a model simulating transient voltage effects paired with experimental stress/rest cycling and in-situ electroluminescence (EL) imaging with voltage monitoring. Our work contributes an important step toward understanding the anomalous performance of perovskite photovoltaics and the factors that influence long-term device reliability.

II. Methodology

A. Experiment Details

Perovskite devices were stressed for 14 hours with 21 stress/rest cycles while simultaneously recording current, voltage, and in-situ EL images. Each cycle consisted of 20 min stress of 15 $mAcm^{-2}$ forward bias followed by 20 min rest at 0 mA constant current at room temperature. Cycling was applied to separate reversible metastability from irreversible degradation. Voltage transients were measured during the stress/rest cycles using a Keithley 2401 sourcemeter. During the stress cycle, a series of 110 EL images were collected with a Princeton Instruments PIXIS camera equipped with a 715 nm long pass filter, which was triggered at specified timepoints through LabVIEW using the voltage output pin of an Arduino Uno microcontroller. To capture varying rates of device evolution, we used three different time intervals to collect images, with the first 40 images spaced 3 s apart, the next 40 images 12 s apart, and the last 30 images 20 s apart. Exposure times were constant for a given device but varied from 20 ms to 100 ms for different devices.

B. Device Simulations

We used device modelling to interpret the experimental voltage transients recorded during constant-current stress/rest cycling. Device simulations were conducted by solving time dependent semiconductor equations (1)-(9). COMSOL Multiphysics® was used to solve the semiconductor equations for electric potential (φ), electron and hole concentrations (n, p), and anion and cation concentrations (C_a, C_c).

$$\frac{\partial}{\partial x}\left(\epsilon_0 \epsilon \frac{\partial \varphi}{\partial x}\right) = -q\rho \quad (1)$$

$$\frac{1}{q}\frac{\partial J_n}{\partial x} - U_n + G = \frac{\partial n}{\partial t} \quad (2)$$

$$J_n = q\mu_n n \frac{\partial \varphi}{\partial x} + qD_n \frac{dn}{dx} \quad (3)$$

$$-\frac{1}{q}\frac{\partial J_p}{\partial x} - U_p + G = \frac{\partial p}{\partial t} \quad (4)$$

$$J_p = q\mu_p p \frac{\partial \varphi}{\partial x} - qD_p \frac{dp}{dx} \quad (5)$$

$$\frac{1}{q}\frac{\partial J_a}{\partial x} + R_a = \frac{\partial C_a}{\partial t} \quad (6)$$

$$J_a = q\mu_a C_a \frac{\partial \varphi}{\partial x} + qD_a \frac{\partial C_a}{\partial x} \quad (7)$$

$$-\frac{1}{q}\frac{\partial J_c}{\partial x} + R_c = \frac{\partial C_c}{\partial t} \quad (8)$$

$$J_c = q\mu_c C_c \frac{\partial \varphi}{\partial x} - qD_c \frac{\partial C_c}{\partial x} \quad (9)$$

The charge density, $\rho = p - n + N_D^+ - N_A^- - C_a + C_c \pm N_t$, includes the donor and acceptor doping, N_D^+ and N_A^-, and charged trap density, N_t. We note that this model reflects the procedures used to understand current-voltage (IV) hysteresis [6]. Key baseline values used for the modeling are listed in Table 1, and additional details can be found in reference [6]. In these devices, we assume mobile anions and stationary cations, which were uniformly distributed at time zero [6]. We varied ion related parameters including ion concentration and anion ion diffusivity to analyze the influence of both parameters toward the voltage transients. Defect densities at the perovskite/ETL (electron transport layer) and perovskite/HTL (hole transport layer) interfaces were set at 10^7 cm^{-2} for this initial model. However, we note that interface defects are an important parameter affecting the performance of perovskite devices [7], and we plan to investigate the effects of interface defects in future studies.

TABLE I. PARAMETERS FOR THE BASELINE MODEL FOLLOWING REF[6].

Parameter	Unit	HTL	Perovskite	ETL
Thickness	nm	170	400	200
Band gap	eV	2.8	1.67	3.6
Electron affinity	eV	2.4	3.9	4.0
Rel. permittivity		3.0	6.5	80
Eff. DOS	cm^{-3}	10^{20}	10^{20}	10^{20}
e/h mobility	cm^2/V s	0.02 / 0.02	0.5 / 0.5	0.02 / 0.02
Doping	cm^{-3}	(p) 8x10^{17}	(p) 8x10^{13}	(n) 8x10^{17}
Mid-gap defects	cm^{-3}	10^{15}	2.6x10^{13}	10^{15}

III. RESULTS AND DISCUSSION

A. Stress/Rest Cycling

Fig. 1 shows the voltage transients during stress/rest cycling for two different types of perovskite devices, which we refer to as V and C type devices. These perovskite cells have a common structure: glass / fluorine-doped tin oxide (FTO) / compact-TiO_2 / mesoporous-TiO_2 / perovskite / spiro-OMeTAD / Au. The V-type cells undergo an additional vapor treatment of the perovskite top surface that is not included in the C-type cells. Over 14 hours of constant-current stress/rest cycling, we observe significant evolution in voltage, although the measured voltages at +3 mA constant current remain within 5% of the initial value. The high-level repeatability of voltage transients for progressive cycles indicates reversible metastabilities that are often attributable to ion motion or charging. However, irreversible degradation also occurs. Overlaying the voltage transients for the progressive cycles on the same time axis (Fig. 1, right) highlights subtle shifts in measured voltage that are not repeatable and continue to evolve from the first to final cycle.

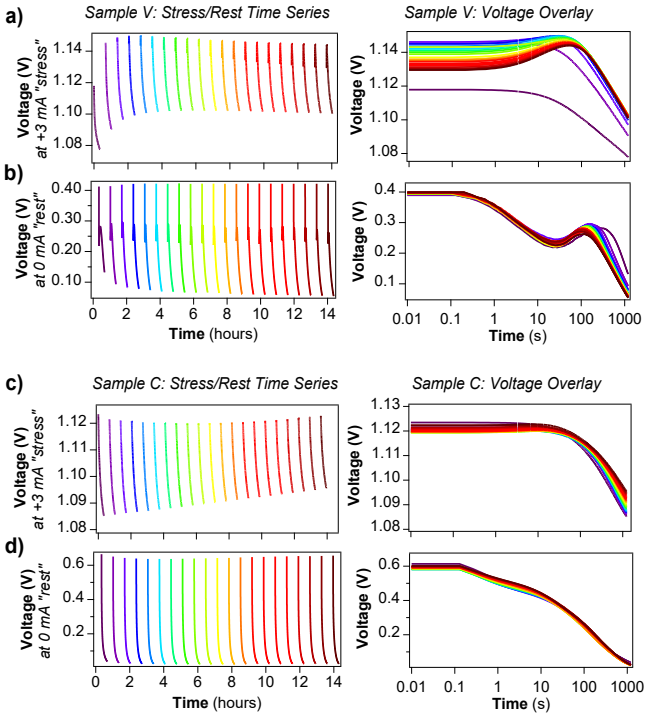

Figure 1. Stress/rest cycling of perovskite devices type V (a-b) and type C (c-d) with voltage transients measured during cycling of constant current bias from +3 mA (a, c) to 0 mA (b, d) over 14 hours and 21 cycles of 20 min stress/rest duration. Right side shows cycles overlaid on a common time axis.

B. Simulations of Voltage Transients

To understand the evolution in voltage transients, we model the voltage over time and vary ion concentration or diffusivity (Fig. 2). For example, both devices in Fig. 1a and 1c (right) show vertical displacements in voltage for subsequent cycles during forward-bias stress in the time range <100 s. This vertical displacement can be understood by referring to our model in Fig. 2a. Fig. 2a shows a time dependent simulation for constant current bias while varying ion density across the different traces. Increasing ion density from 2x10^{17} cm^{-3} to 4x10^{18} cm^{-3} results in a vertical shift in modeled transients for the time range <100 s. Interestingly, the voltage initially increases with increasing ion density, but there is a threshold around 1.161V for 2x10^{18} cm^{-3} where the voltage then slightly decreases with further increases in ion density. For the time range >100 s, the model suggests a faster voltage decline with increasing ion density. Based on these simulations, we hypothesize that the effective mobile ion density may be decreasing for progressive cycles in our devices, possibly caused by ion re-distribution, charge compensation, or ion-consuming chemical reactions.

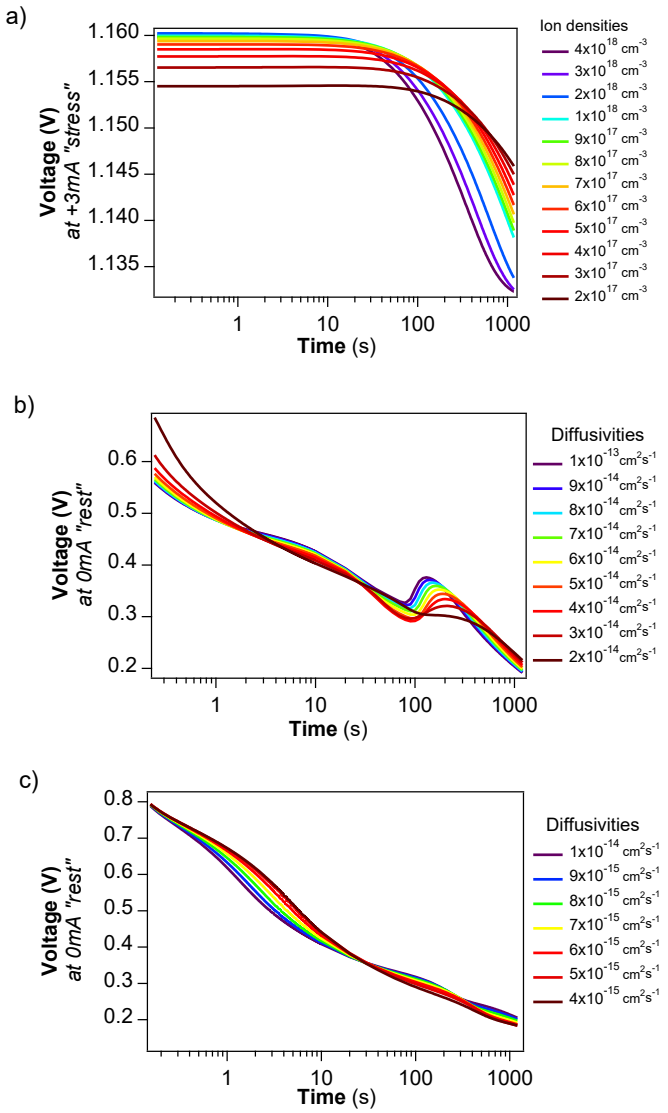

Figure 2. Simulated effects of (a) ion density at ion diffusivity of 10^{-14} cm^2s^{-1} and (b-c) ion diffusivity (D_a) at ion density of 10^{17} cm^{-3} on voltage transients for (a) constant-current forward bias and (b-c) 0 mA constant current recovery.

Ion diffusivity also affects the voltage transients in addition to the ion concentration. The effects of diffusivity are most clearly demonstrated in the voltage recovery transients at 0 mA (Fig. 1b and Fig. 1d). We model the effects of anion diffusivity (D_a) in Fig. 2b and Fig. 2c. We observe two different ranges of D_a that mirror our experimental data for either the V-type or C-type perovskite devices. That is, D_a from $2x10^{-14}$ cm^2s^{-1} to $1x10^{-13}$ cm^2s^{-1} shows a pronounced voltage overshoot after ~100 s of recovery (Fig. 2b), similar to the V-type device in Fig. 1b. In the model, increasing diffusivity causes a shift in the overshoot to earlier times (shift overshoot to the left). This is similar to the experimental data, which shows a voltage overshoot shifting to earlier times for later cycles. We interpret this model to possibly suggest increasing ion diffusivity during device burn-in over many hours of cycling. Greater agreement between the data and model may be obtained by simultaneously varying the effective ion concentration. Indeed, our analysis of the "stress" cycles (Fig. 1a and 2a) suggested decreasing ion concentration, which may account for the decreasing magnitude of the voltage overshoot at later cycles in Fig. 1b.

The lower range of D_a values (D_a <$1x10^{-14}$ cm^2s^{-1}) resulted in a suppressed voltage overshoot (Fig. 2c). The simulations in this D_a range appear similar to the experimental voltage recovery transients for the C-type device in Fig. 1d. We note that simulated transients with a suppressed voltage overshoot can be obtained at lower (D_a < $1x10^{-14}$ cm^2s^{-1}) ranges of diffusivity for the parameters that we use in our model. However, further studies are needed to determine the D_a range that applies to our devices.

C. In-Situ Electroluminescence Imaging

Importantly, the analysis thus far has focused on the bulk voltage output of the devices without considering spatial inhomogeneities or defective regions that may exist across the device area. To understand spatially-distributed effects, we collect EL images throughout the stress/rest cycling represented in Fig. 1. EL images can be understood as a map of the cell voltage, where EL is exponentially proportional to internal voltage. EL imaging is commonly used for troubleshooting reliability issues in commercial PV technologies [8-10], and it will become especially important in perovskites as perovskite devices increase in size and approach the goal of commercialization.

Fig. 3 shows representative in-situ EL images collected over the course of stress cycling for a Type V device (subset of 110 images per cycle). We observe evolving EL spatial distribution from first to last image within a given cycle, as well as from earlier to later cycles. The reproducible changes that occur within each cycle from image 1 to image 110 represent reversible metastabilities, while any progressive changes from cycle 1 to cycle 21 represent irreversible degradation. For example, we observe a reversible change where a pattern of dark diagonal stripes exists in image 1 of cycles 5-21, and it is no longer visible in image 110 of cycles 5-21 (i.e. after the 20 minute constant current stress). We observe irreversible changes that include an overall increase (or decrease) in the average magnitude of EL signal in image 110 (or image 1) when progressing to the final stress cycle.

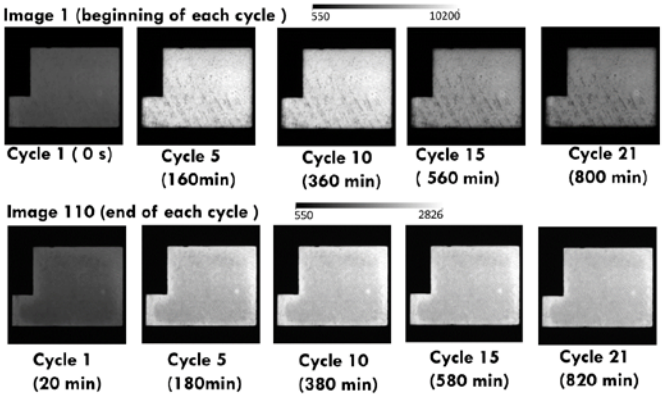

Figure 3. Example of un-processed electroluminescence images at the beginning (top) and end (bottom) of selected stress cycles for a type V device.

To better understand the subtle features of evolving EL images during stress cycling, we compare the transient EL

intensity with the voltage transients discussed in Section A. Fig. 4 shows the EL mean value averaged across the device overlayed with the corresponding voltage trace for cycle 1 (a) and cycle 21 (b). During the first cycle, Fig. 4a shows that the EL transient follows the voltage, as expected. This corresponds to a minimal spatial change in EL images over the course of the cycle. That is, we observe uniform cell area in divided images that compare image 16 to image 1, or image 110 to image 16, as plotted in Fig. 4a (right). Note that the image background represents an unchanged value equal to 1, so the general darkening of the divided cell area in the images with respect to background corresponds to an overall decrease in EL intensity.

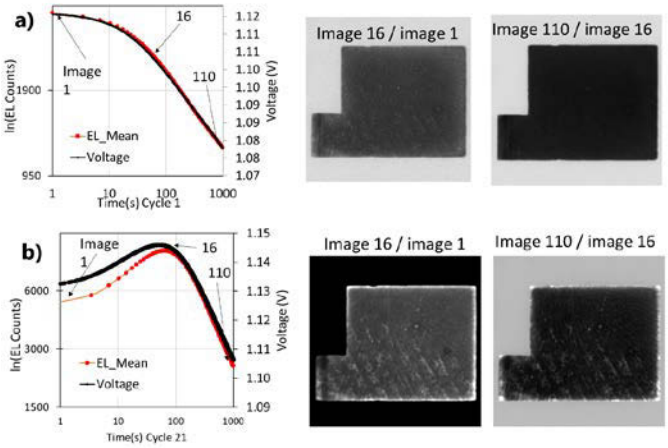

Figure 4. Comparison of EL and voltage transients for cycle 1 and 21 for type V device are shown on 4a and 4b. Images on the right show image processing results responsible for EL and voltage deviations.

For the later stress cycles (e.g. cycle 21 in Fig. 4b), the EL transient deviates from the voltage. Dividing the images highlights regions that do not follow the voltage trend. For example, dividing image 16 by image 1 as in Fig. 4b (right) shows edge regions and defective areas with relative EL brightening compared to the majority of the device area. Interestingly, dividing the last image (110) by image 16 suggest that the cell edges and defective areas continue to brighten in EL even as the main device area follows the voltage and decreases in intensity.

Fig. 5 shows a similar imaging analysis for a Type C device (corresponding to the device stressed in Fig. 1 c-d). In this case, the spatially-averaged EL transients deviate more substantially from the voltage trends. This deviation correlates with more inhomogeneities in the EL images. Even in the first cycle (Fig. 5a) the divided images highlight separate mid-cell phases with either EL brightening or darkening. During the last cycle (Fig. 5b), we observe relative brightening of cell edges and scratches, reminiscent of the effects observed in Fig. 4b for the later cycles in Type V device. With relatively low inhomogeneities in the EL images at the last cycle, the V type device showed to be more stable with the stressing. In addition to the EL images to spatially resolve nonuniform evolution, further microscopic characterizations such as atomic force microscopy-based, scanning electron microscopy-based techniques will be performed on the area of interest.

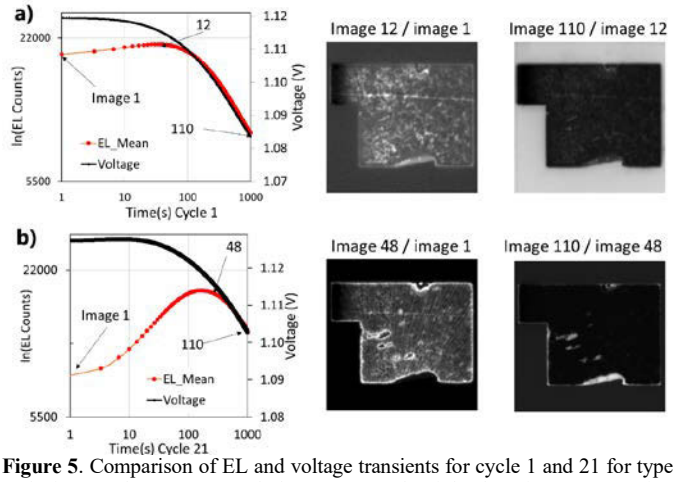

Figure 5. Comparison of EL and voltage transients for cycle 1 and 21 for type C device are shown on 5a and 5b. Images on the right show image processing results responsible for EL and voltage deviations.

IV. Conclusions

The imaging results and analysis procedures presented here highlight the importance of collecting a series of EL images to understand perovskite (meta)stability rather than using single-time-point images. Both the intensities and spatial distributions of single-time-point images are unreliable due to the dynamic nature of luminescence and voltage in perovskites. The spatial deviations in EL images highlight regions that may require further microscopic study to mitigate reliability concerns.

Furthermore, we presented a model that can be used to simulate the transient voltage behavior and understand the roles of ion concentration and diffusivity. In future studies, we aim to gain insight into spatially-distributed ion effects and underlying causes of the deviating voltage versus EL intensity by applying our model to dissimilar regions of the EL images.

V. Acknowledgment

This work was authored in part by the National Renewable Energy Laboratory, operated by Alliance for Sustainable Energy, LLC, for the U.S. Department of Energy (DOE) under Contract No. DE-AC36-08GO28308. Funding provided by U.S. Department of Energy Office of Energy Efficiency and Renewable Energy Solar Energy Technologies Office. The views expressed in the article do not necessarily represent the views of the DOE or the U.S. Government.

The U.S. Government retains and the publisher, by accepting the article for publication, acknowledges that the U.S. Government retains a nonexclusive, paid-up, irrevocable, worldwide license to publish or reproduce the published form of this work, or allow others to do so, for U.S. Government purposes.

References

[1] "Best Research-Cell Efficiency Chart." https://www.nrel.gov/pv/cell-efficiency.html (accessed Jan. 22, 2021)

[2] J. Mizusaki et al., "Ionic conduction of the perovskite-type halides," Solid State Ionics, vol. 11, no. 3, pp. 203–211, Nov. 1983.

[3] H. J. Snaith et al., "Anomalous Hysteresis in Perovskite Solar Cells," J. Phys. Chem. Lett., vol. 5, no. 9, pp. 1511–1515, May 2014.

[4] Z. Xiao et al., "Efficient, high yield perovskite photovoltaic devices grown by interdiffusion of solution-processed precursor stacking layers," Energy Environ. Sci., vol. 7, no. 8, pp. 2619–2623, Jul. 2014.

[5] B. Chen et al., “Impact of Capacitive Effect and Ion Migration on the Hysteretic Behavior of Perovskite Solar Cells,” J. Phys. Chem. Lett., vol. 6, no. 23, pp. 4693–4700, Dec. 2015.

[6] S. van Reenen et al., “Modeling Anomalous Hysteresis in Perovskite Solar Cells,” J. Phys. Chem. Lett., vol. 6, no. 19, pp. 3808–3814, Oct. 2015.

[7] S. Shao et al S., “The Role of the Interfaces in Perovskite Solar Cells”. Adv. Mater. Interfaces 2020, 7.

[8] Johnston, S. et al “From Modules to Atoms: Techniques and Characterization for Identifying and Understanding Device-Level Photovoltaic Degradation Mechanisms.” 2019.

[9] Sulas-Kern D.B. et al., "Fill Factor Loss in Fielded Photovoltaic Modules Due to Metallization Failures, Characterized by Luminescence and Thermal Imaging," 2019 IEEE 46th Photovoltaic Specialists Conference (PVSC), 2019.

[10] Owen-Bellini, M. et al. “Methods for In Situ Electroluminescence Imaging of Photovoltaic Modules Under Varying Environmental Conditions” Journal of Photovoltaics, 2020.